Macromolecular Rapid Communication
www.mrc-journal.de

Electrochromic Response Capability Enhancement with Pentiptycene-Incorporated Intrinsic Porous Polyamide Films

Ya-Wen Chiu, Wei Shyang Tan, Jye-Shane Yang, Min-Hao Pai, and Guey-Sheng Liou**

Enhancing switching response capability of electrochromic (EC) polymers has been a topical issue. Herein, the H-shaped nonplanar pentiptycene scaffold is successfully introduced into the polyamide film derived from *N*,*N*′-bis(4-aminophenyl)-*N*,*N*′-di(methoxyphenyl)-1,4-phenylenediamine (TPPA), and the resulting copolymer shows enhanced EC behaviors, including lower oxidation potential and shorter switching response time, as compared to the corresponding TPPA-derived homopolymer.

The electrochromic (EC) behaviors of triphenylamine (TPA)-derived polymers have been investigated by one of our groups since 2005.[1] These polymers usually display high transparency at the neutral state and undergo multiple color changes during the redox processes. The number of coloring states depends on the number of oxidation centers in the polymers. An ideal EC polymer should not only have high color contrast ratio, large coloration efficiency, shorter response time, and longer cycle life but also have low oxidation voltage, good environmental stability, and diverse colors.[2] To achieve high color contrast, controlling the film thickness is a direct approach; however, thicker films often cause longer switching time and shorter cycle life.[3] Previous attempts to solve the dilemma are to prepare porous polymer films or nanostructured materials[4] and to employ organic–inorganic hybrids.[5] Herein, we report a new approach to enhance the switching response capability by incorporating the pentiptycene scaffold into the polymer chain.

Pentiptycene belongs to the family of iptycene, which contains phenylene and bicyclo[2,2,2]octatriene units.[6] The simplest form of iptycene is triptycene, which contains V-shaped cavities, whereas pentiptycene contains not only V-cavities but also U-cavities. These cavities create internal molecular free volume (IMFV), which has introduced intriguing properties to π-conjugated polymers. As depicted in **Figure 1**, a high fraction of the pentiptycene unit in the backbone could effectively prevent π-stacking among polymer chains to retain a high photoluminescence quantum efficiency of the polymer films and to form intrinsic pores for accommodating small molecules.[7] In addition, one of our groups recently demonstrated that a low fraction (below 5%) of pentiptycene incorporation in the polyaniline backbone could significantly enhance the electrochemical capacity and stability of the polymer films, attributable to the "molecular clipping effect" that confines the neighboring polymer chains.[8] In this context, we have explored the *N*,*N*′-di(methoxyphenyl)-1,4-phenylenediamine (TPPA)-based EC polyamides that contain the pentiptycene scaffold. We envisaged that the intrinsic pores created by the pentiptycene groups could promote diffusion rate of counterions in the polymer matrix and that the clipping effect could facilitate electron transfer among the polymer chains and, therefore, an enhanced EC switching capability might be achieved.

The synthesis of the TPPA-based polyamide (TPPA-cyclo) and pentiptycene-containing copolyamide (TPPA/penti-cyclo) was carried out by direct polycondensation of 1,4-cyclohexanedicarboxylic acid and the corresponding TPPA (**Scheme 1**). Their intrinsic viscosities and molecular weights are summarized in Table S1, Supporting Information, and their solubility behaviors are shown in Table S2, Supporting Information. The weight-average molecular weight (M_w) and polydispersity (M_w/M_n), estimated by gel permeation chromatography, were 53 700 (1.50) for TPPA-cyclo, and 10 400 (1.41) for TPPA/penti-cyclo. Thermal properties measured by thermogravimetric analysis and differential scanning calorimetry (DSC) are shown in Figures S1 and S2, Supporting Information, and the related values are listed in Table S3, Supporting Information. Both polymers possessed good thermal stability without presenting significant weight loss up to 350 °C. Furthermore, TPPA/penti-cyclo displayed higher stability, which could be attributed to the introduction of pentiptycene moieties. The DSC trace showed that the glass transition temperature of TPPA-cyclo was around 250 °C, while TPPA/penti-cyclo did not give an obvious change

Y.-W. Chiu, M.-H. Pai, Prof. G.-S. Liou
Institute of Polymer Science and Engineering
National Taiwan University
No. 1, Sec. 4, Roosevelt Rd., Taipei 10617, Taiwan
E-mail: gsliou@ntu.edu.tw
Dr. W. S. Tan, Prof. J.-S. Yang
Department of Chemistry
National Taiwan University
No. 1, Sec. 4, Roosevelt Rd., Taipei 10617, Taiwan
E-mail: jsyang@ntu.edu.tw
Prof. G.-S. Liou
Advanced Research Center for Green Materials Science and Technology
National Taiwan University
Taipei 10617, Taiwan
The ORCID identification number(s) for the author(s) of this article can be found under https://doi.org/10.1002/marc.202000186.

DOI: 10.1002/marc.202000186

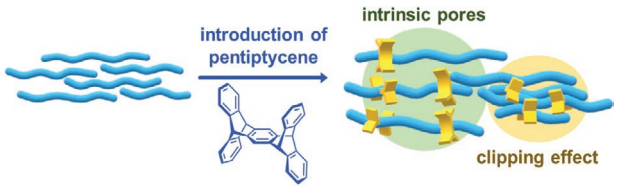

Figure 1. Illustration of the formation of intrinsic pores and clipping effect by introducing pentiptycene structures into polymer chains.

up to 350 °C. The NMR spectrum of TPPA/penti-cyclo is shown in Figure S3, Supporting Information. According to the NMR signals, the molar ratio of the TPPA versus the pentiptycene unit is about 5:3. Because the pentiptycene unit is not EC-active, TPPA/penti-cyclo would contain fewer amounts of the EC units than TPPA-cyclo under the same materials loading. Therefore, two types of TPPA/penti-cyclo films differing in thickness, on the basis of the optical density, were prepared to study the effects of pentiptycene on the EC performance: the first type has a similar film thickness as the TPPA-cyclo films (330 ± 30 vs 310 ± 15 nm), and the second type is roughly two times thicker (630 ± 55 nm) than the first type to have a similar loading of EC units to TPPA-cyclo. The two types of films are named as TPPA/penti-thin and TPPA/penti-thick, respectively, and the corresponding UV–vis transmittance spectra are shown in Figure S4, Supporting Information. The film transparency is similar for the TPPA-cyclo and TPPA/penti-thin films, and they are higher than the TPPA/penti-thick films.

The electrochemical properties of TPPA-cyclo, TPPA/penti-thin, and TPPA/penti-thick films coated on indium tin oxide (ITO) glasses were measured by cyclic voltammetry (CV) to obtain the oxidation redox potentials. The CV diagrams are illustrated in **Figure 2**, and the related values are summarized in **Table 1**. The oxidation potentials of TPPA/penti-thin at the first and the second oxidation states (0.23 and 0.63 V) were both lower than those of TPPA-cyclo films (0.33 and 0.75 V), indicating that the EC materials can be oxidized more easily in the presence of the pentiptycene units. Moreover, the oxidation redox potentials of TPPA/penti-thick (0.27 and 0.68 V) are also smaller than those of TPPA-cyclo films. Furthermore, the potential difference between the oxidation and the reduction peaks, ΔE, at the two oxidation states revealed the same tendency as the oxidation potentials. These results demonstrate the positive effects of the pentiptycene moieties on the enhancement of electrochemical response capability. This might be attributed to a less dense packing of polymers in TPPA/penti-thin and TPPA/penti-thick as compared with that in TPPA-cyclo film such that the formation of intrinsic pores

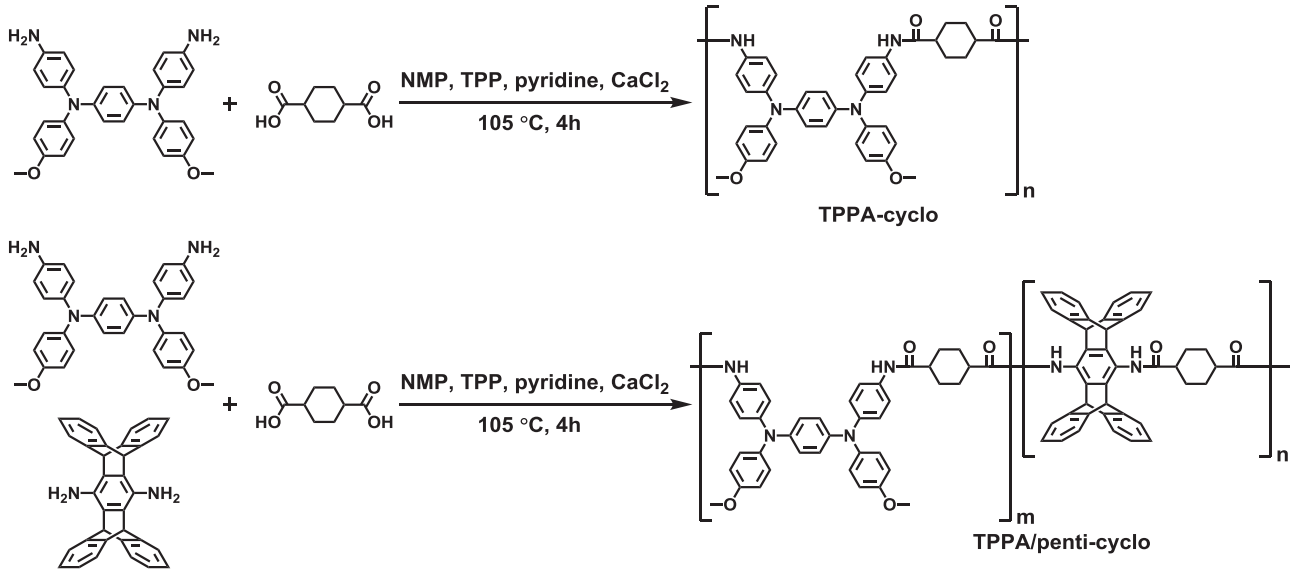

Scheme 1. Synthesis routes of TPPA-cyclo and TPPA/penti-cyclo.

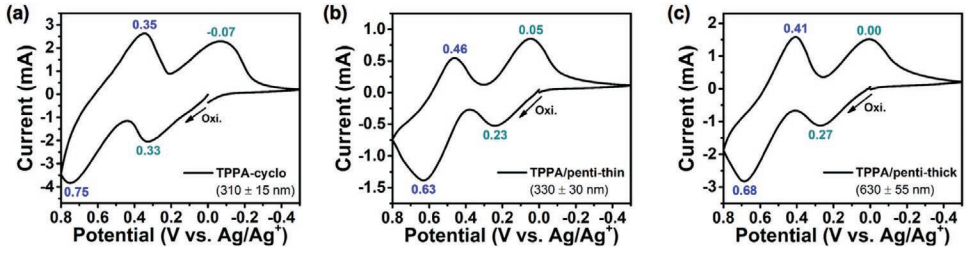

Figure 2. Cyclic voltammograms of a) TPPA-cyclo (thickness: 310 ± 15 nm), b) TPPA/penti-thin (thickness: 330 ± 30 nm), and c) TPPA/penti-thick (thickness: 630 ± 55 nm) films on the ITO-coated glass substrate (coated area: 0.6 cm × 3 cm) in 0.1 M $TBABF_4$/MeCN at a scan rate of 50 mV s^{-1}.

Table 1. Redox potentials and impedance data of the prepared films.

Polymers[a]	First oxidation state			Second oxidation state			0.35 V (coloring state)		0 V (bleaching state)	
	$E_{oxi.}$[b] [V]	$E_{red.}$[c] [V]	ΔE[d] [V]	$E_{oxi.}$[b] [V]	$E_{red.}$[c] [V]	ΔE[d] [V]	R_{Ω}[e] [Ω]	R_{ct}[f] [Ω]	R_{Ω}[e] [Ω]	R_{ct}[f] [Ω]
TPPA-cyclo	0.33	–0.07	0.40	0.74	0.38	0.36	3.98	24.9	4.09	25.5
TPPA/penti-thin	0.23	0.05	0.18	0.63	0.46	0.17	3.28	18.6	3.41	18.9
TPPA/penti-thick	0.27	0.00	0.27	0.68	0.41	0.27	3.68	24.2	3.31	26.9

[a]Measured relative to Ag/Ag^+ in MeCN; [b]Potentials at the oxidation peaks; [c]Potentials at the reduction peaks; [d]Potential differences between oxidation and reduction peaks = $|E_{oxi.} - E_{red.}|$; [e]Solution resistance, obtained from interception of the Nyquist plots on the real axis; [f]Charge transfer resistance, obtained from the diameter of the arc.

among polymer chains facilitates the diffusion of counterions in the polymer matrix more efficiently. This also explains the lower driving force and applied voltage for the oxidation of the pentiptycene-containing polymers.

Spectroelectrochemical spectra of these EC polymer films were shown in **Figure 3**. Although the TPPA-based polyamides have two oxidation states, the first oxidation state should be a judicious choice for practical application because of the lower

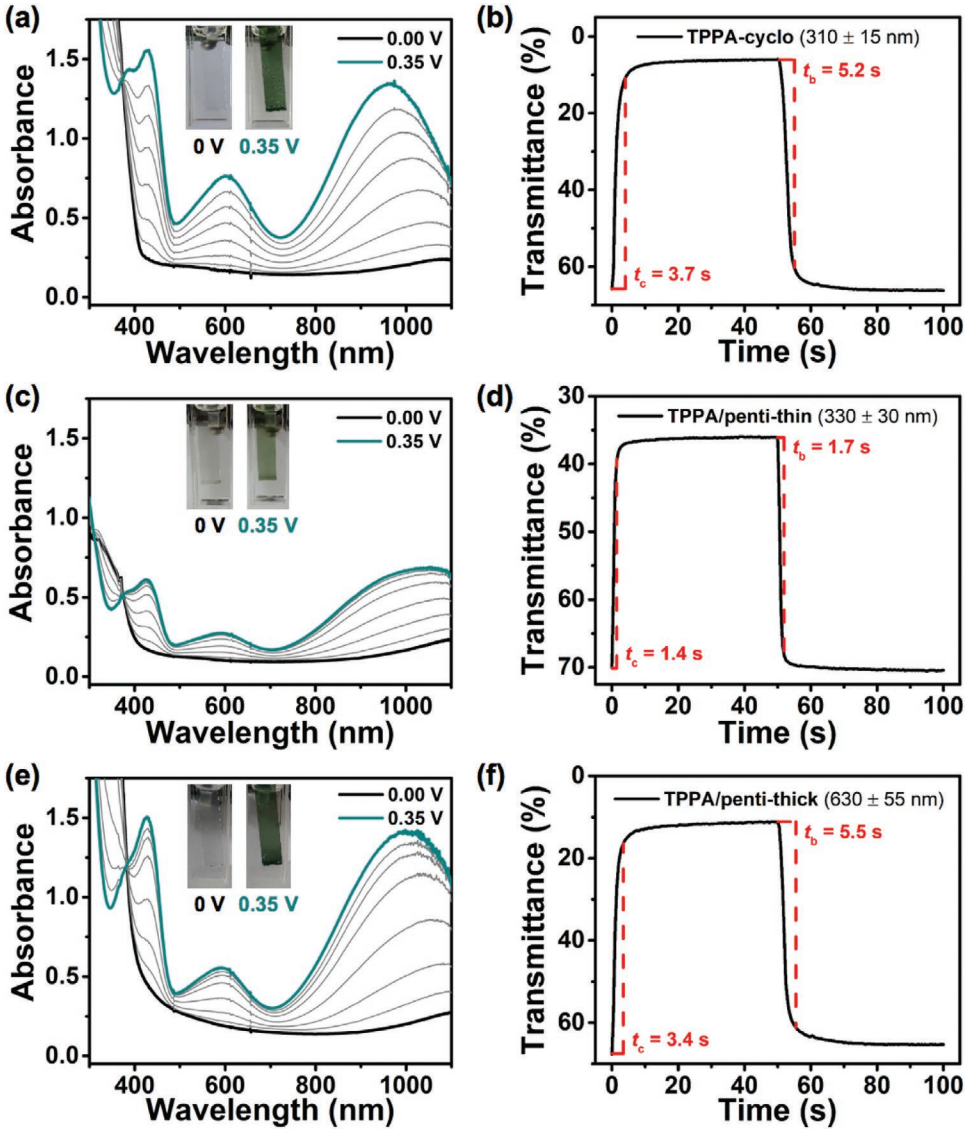

Figure 3. Spectroelectrochemical spectra and switching response time (0.35 V as coloring voltage and –0.1 V as bleaching voltage) of a,b) TPPA-cyclo (thickness: 310 ± 15 nm), c,d) TPPA/penti-thin (thickness: 330 ± 30 nm), and e,f) TPPA/penti-thick (thickness: 630 ± 55 nm) films on the ITO-coated glass substrate (coated area: 0.6 cm × 3 cm) in 0.1 M $TBABF_4$/MeCN.

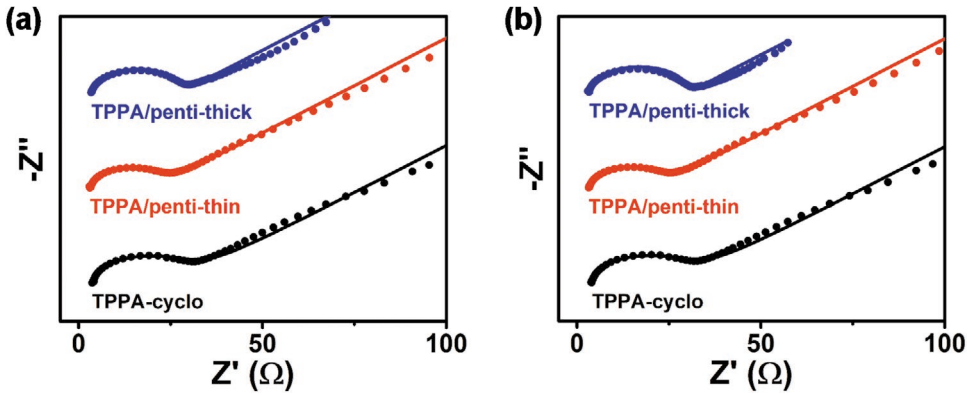

Figure 4. Nyquist plots of TPPA-cyclo (thickness: 310 ± 15 nm), TPPA/penti-thin (thickness: 330 ± 30 nm), and TPPA/penti-thick (thickness: 630 ± 55 nm) films on ITO glasses (coated area: 0.6 cm × 3 cm) in 0.1 M $TBABF_4$/MeCN at a) 0.35 V and b) 0 V.

oxidation potential and higher stability. Thus, the EC behavior was investigated only at the first oxidation state in the experiments. According to Figure 2, the applied voltage was at 0.35 V for coloring and at –0.10 V for bleaching. As illustrated in Figure 3, the characteristic absorption peaks of TPPA-cyclo and TPPA/penti-cyclo at the first oxidation state were at 430 and 600 nm, corresponding to the color of green grass. The relative absorbance is in the order TPPA/penti-thick ~ TPPA/cyclo > TPPA/penti-thin, which reflects the relative amount of the EC-active moieties in the polymers. Regarding the response time, it took TPPA-cyclo films 3.7 s to reach 90% of total switching transmittance change from the neutral state to the coloring state, and 5.2 s to bleach from the oxidized state to the original neutral state. In contrast, TPPA/penti-thin exhibited shorter response times, only 1.4 s for coloring and 1.7 s for bleaching and highlighting the pentiptycene effect (recall that the thickness of TPPA-cyclo and TPPA/penti-thin is similar). Again, an enhancement in the diffusion rate for the counterions in the polymer matrix during the EC operations might account for the pentiptycene effect. This argument is further supported by the performance of TPPA/penti-thick with the coloring time and bleaching time being 3.4 and 5.5 s, respectively. Since the thickness of TPPA/penti-thick is nearly double of that of TPPA-cyclo, their similarities in the response times unambiguously demonstrate the promising pentiptycene effects on EC switching capability.

Electrochemical impedance spectroscopy (EIS) was also employed to investigate the electroactivity and conductivity of the polymer films coated on the electrode.[9] The results of EIS are shown in **Figure 4**. The data were fitted by the classical Randles four-element circuit. The solution resistance (R_Ω) was obtained from the intercept of horizontal axis, and the charge transfer resistance (R_{ct}) from the diameter of the semi-circle or the arc. The values of R_{ct} and R_Ω for the coloring (0.35 V) and for the bleaching (0.0 V) states are summarized in Table 1. At the coloring potential, the R_{ct} values of TPPA-cyclo, TPPA/penti-thin, and TPPA/penti-thick are 24.9, 18.6, and 24.2 Ω, respectively. Similar R_{ct} values are also observed for the three polymers in the bleaching process, that is, 25.5, 18.9, and 26.9 Ω for TPPA-cyclo, TPPA/penti-thin, and TPPA/penti-thick, respectively. Since a lower R_{ct} value implies a higher diffusion rate of the counterions, the relative R_{ct} values of the three polymer films again support the proposition that the pentiptycene effect on shortening the switching response time is due to enhanced ion diffusion in the polymer matrix during the redox operations.

In conclusion, the incorporation of pentiptycene units into TPPA-based EC polymers could significantly improve the EC performance of the polymers. More specifically, with the same film thickness, the first oxidation potentials were lowered from 0.33 to 0.23 V, the Δ*E*s from 0.40 to 0.27 V, and the response time were shortened from 3.7/5.2 to 1.4/1.7 s for coloring and bleaching procedures. Such an intriguing pentiptycene effect is attributed to the intrinsic pores formed by the IMFV of the pentiptycene units, giving a promising material that could be applied for further applications on electrochromism.

Supporting Information

Supporting Information is available from the Wiley Online Library or from the author.

Acknowledgements

This work was financially supported by the "Advanced Research Center for Green Materials Science and Technology" from the Featured Area Research Center Program within the framework of the Higher Education Sprout Project by the Ministry of Education (108L9006) and the Ministry of Science and Technology in Taiwan (MOST 108-3017-F-002-002, 107-2113-M002-022-MY3, 107-2113-M-002-024-MY3, and 107-2221-E-002-066-MY3).

Conflict of Interest

The authors declare no conflict of interest.

Keywords

electrochromism, intrinsic porous structure, pentiptycene, polyamide films, switching response

Received: April 6, 2020
Revised: April 24, 2020
Published online:

[1] a) S. H. Cheng, S. H. Hsiao, T. H. Su, G. S. Liou, *Macromolecules* **2005**, *38*, 307; b) H. J. Yen, G. S. Liou, *Polym. Chem.* **2018**, *9*, 3001.

[2] a) A. A. Argun, P. H. Aubert, B. C. Thompson, I. Schwendeman, C. L. Gaupp, J. Hwang, N. J. Pinto, D. B. Tanner, A. G. MacDiarmid, J. R. Reynolds, *Chem. Mater.* **2004**, *16*, 4401; b) A. L. Dyer, A. M. Österholm, D. E. Shen, K. E. Johnson, J. R. Reynolds, in *Electrochromic Materials and Devices* (Eds: R. J. Mortimer, D. R. Rosseinsky, P. M. S. Monk), Wiley-VCH, Weinheim, Germany **2013**, p. 113; c) R. J. Mortimer, A. L. Dyer, J. R. Reynolds, *Displays* **2006**, *27*, 2.

[3] H. S. Liu, B. C. Pan, D. C. Huang, Y. R. Kung, C. M. Leu, G. S. Liou, *NPG Asia Mater.* **2017**, *9*, e388.

[4] a) B. C. Pan, W. H. Chen, S. H. Hsiao, G. S. Liou, *Nanoscale* **2018**, *10*, 16613; b) S. Xiong, P. S. Lee, X. Lu, in *Electrochromic Materials and Devices* (Eds: R. J. Mortimer, D. R. Rosseinsky, P. M. S. Monk), Wiley-VCH, Weinheim, Germany **2013**, p. 249.

[5] a) B. C. Pan, W. H. Chen, T. M. Lee, G. S. Liou, *J. Mater. Chem. C* **2018**, *6*, 12422; b) V. K. Thakur, G. Ding, J. Ma, P. S. Lee, X. Lu, *Adv. Mater.* **2012**, *24*, 4071; c) S. Xiong, S. L. Phua, B. S. Dunn, J. Ma, X. Lu, *Chem. Mater.* **2010**, *22*, 255.

[6] J. S. Yang, J. L. Yan, *Chem. Commun.* **2008**, 1501.

[7] a) J. S. Yang, T. M. Swager, *J. Am. Chem. Soc.* **1998**, *120*, 5321; b) J. S. Yang, T. M. Swager, *J. Am. Chem. Soc.* **1998**, *120*, 11864.

[8] W. S. Tan, T. Y. Lee, Y. F. Hsu, S. J. Huang, J. S. Yang, *Chem. Commun.* **2018**, *54*, 5470.

[9] M. E. Orazem, B. Tribollet, *Electrochemical Impedance Spectroscopy*, Wiley, Hoboken, NJ **2017**, p. 243.

